

Orbital Control for Swimming in Underwater Snake Robots using Energy-Shaping and Consensus Control*

Mads Erlend Bøe Lysø¹, Elena Panteley², Kristin Y. Pettersen¹ and Jan Tommy Gravdahl¹

Abstract—In this paper, we present a controller for stabilizing and synchronizing a set of phase-shifted oscillations in a system of n double integrators. The motivating application is the control of swimming locomotion in an underwater snake robot. The oscillations are stabilized to a desired amplitude and frequency, and synchronized to achieve a desired phase shift between each oscillator. The result is a controller which stabilizes the desired gait while avoiding the undesirable transient behavior (colloquially known as "catching-up"-effects) associated with the tracking-based methods which are currently prevalent in the field. The controller is based on energy-shaping control and consensus control, and it is shown to render the desired orbit almost globally asymptotically stable. The emergence and stability of the desired behavior is demonstrated in a simulation study.

Index Terms—Nonlinear marine systems control, Autonomous underwater vehicles, Synchronization, Distributed control

I. INTRODUCTION

Understanding and mastering operations in underseas environments is a critical part of facing the challenges of the future. Through practices like maritime freight transport and aquaculture, as well as through critical undersea infrastructure for telecommunication and power transmission, substantial parts of the global economy take place in marine environments. In order to harness the benefits of automation in such industries, it is necessary to develop and build autonomous underwater robots which are safe and energy-efficient.

A promising research avenue is that of underwater snake robots (USRs), a type of articulated intervention autonomous underwater vehicle (AIAUV) built from narrow links connected by revolute joints [1]–[3]. One benefit of USRs is their ability to locomote by swimming, mimicking eel-like gait patterns [4]. In particular, a gait pattern denoted lateral undulation has been used and researched extensively in the USR literature.

A typical approach to stabilizing such gaits is through the method of closed-loop reference trajectory tracking. One

example is found in [5], where a PD-controller was utilized to track a reference swimming gait for a snake-like robot in simulations and experiments. The paper found moderate discrepancies ($< 20\%$) between the simulations and experimental data. Another example is found in [6], where a joint controller was designed for achieving a lateral undulation gait pattern in a USR, based on trajectory tracking. The controller was designed through the method of integrator backstepping, and found to render the tracking error of the closed-loop system uniformly globally exponentially stable (UGES). Furthermore, the overall system was analyzed through a cascaded systems approach. A slightly different but related approach can be found in [7], where a controller for achieving lateral undulation in a USR was designed as a set of virtual holonomic constraints (VHCs) which evolved with time. The controller which was employed was found, based on analysis from [8], to locally exponentially stabilize the VHC manifold. In [9], a lateral undulation trajectory was similarly encoded through time-varying VHCs, and the body shape of a planar snake robot was stabilized to the VHC manifold. Furthermore, a modified super-twisting sliding-mode controller was employed to stabilize the head angle and forward velocity to desired values in a simulation with parameter uncertainties. Whether the trajectories are given directly or whether they are encoded through a set of VHCs, the reference trajectory is a set of periodic signals which are phase shifted, and which are evolving either with time or with another flow variable.

However, while the reference trajectory tracking approach has been successfully applied for gait stabilization in the literature, it has certain drawbacks. One could argue that if the control objective is the generation and stabilization of a gait, the absolute phase of the resulting gait is not relevant: That is, two periodic behaviors which are identical up to a phase shift can be said to equally achieve the control objective. This may be phrased as a problem of orbital stabilization, with the desired orbit determining the gait. However, when using a trajectory tracking controller, the absolute phase of the reference signal becomes relevant. This implies that while the gait is an attractive set for the closed-loop system, it is not an orbit, as it is possible for the state to originate in the set and subsequently exit. This can be seen through "catching-up" behavior where the system state, if it lags behind the reference, will speed up to drive the tracking error to zero, as illustrated in [10]. Thus, utilizing a trajectory-tracking controller for an orbital stabilization problem is potentially problematic.

A different approach to the problem of gait generation is to

*This result is part of a project that has received funding from the European Research Council (ERC) under the European Union's Horizon 2020 research and innovation programme, through the ERC Advanced Grant 101017697-CRÈME.

¹M. E. B. Lysø, K. Y. Pettersen and J. T. Gravdahl are with Department of Engineering Cybernetics, Norwegian University of Science and Technology, O. S. Bragstads plass 2D Trondheim, Norway {mads.e.b.lyso, kristin.y.pettersen, jan.tommy.gravdahl}@ntnu.no

²E. Panteley is with Laboratoire des signaux et systèmes, CNRS, 3 rue Joliot Curie 91190 Gif sur-Yvette, France elena.panteley@l2s.centralesupelec.fr

utilize the method of pattern formation using central pattern generators (CPGs). There is a wide body of literature on CPGs. In [11], a CPG was used to generate a gait pattern for serpentine locomotion for a snake-like robot. Multiple gaits were achieved in simulation and verified experimentally. In [12], a CPG was utilized for the locomotion of a snake-like robot, and a parameter search was performed using a genetic algorithm in order to optimize over movement speed and battery consumption when locomoting on a soft floor. The resulting parameters were verified both in simulation and experimentally. Similarly, in [13] a CPG approach was employed, and adapted to different ground friction coefficients using a genetic algorithm. The results were verified in simulation.

However, while experimental validation of CPG approaches is common throughout the literature, performing a mathematical stability analysis of the complete system is very difficult, and is typically not done [14]. Furthermore, while the CPG itself is formulated as a set of dynamical systems achieving synchronized oscillatory behavior, this only applies on the kinematic level. In order for the dynamical system to exhibit the desired behavior, the signal from the CPG will be considered as a reference trajectory to be tracked. Thus, the previously mentioned challenges of trajectory tracking methods apply here as well.

In [15], a controller based on energy-shaping was proposed to generate and stabilize a lateral undulation swimming pattern in a USR without the use of a reference trajectory. The resulting controller was shown numerically to render the gait locally orbitally exponentially stable in the sense of Poincaré, for a range of control parameters. Furthermore, the controller was demonstrated through simulations to be more robust to unmodelled disturbances than an existing reference trajectory tracking controller from the literature.

In the study of networked dynamical systems, synchronization occurs when the trajectory of each subsystem is identical but potentially time shifted. In [16], a framework was introduced for analyzing the synchronization of interconnected dynamical systems. It was found that the analysis of such system can be reformulated as the analysis of two systems evolving on orthogonal subspaces, where one characterizes the mean-field behavior of the system while the other characterizes the synchronization errors. In [17], a system of N identical interconnected nonlinear oscillators was analyzed, and it was found that the behavior of the system approaches that of a single oscillator under a sufficiently high coupling strength. However, the systems converge to a single identical oscillation, with no phase shift. Furthermore, the studied case assumes control authority in all system states.

As shown in [18], the joint dynamics of a USR under a feedback-linearizing controller can be reduced to a set of n double integrators. Thus, the problem of achieving lateral undulatory swimming for a USR can be reformulated as stabilizing a set of phase-shifted oscillations of a desired frequency and amplitude in such a system.

We may then state the research question addressed in this paper as follows: How to stabilize a set of phase-shifted

oscillations such as those found in the lateral undulation gait, where control authority is only found on the acceleration level, in a manner which avoids the "catching-up" behavior and other potential shortcomings of tracking methods, while proving non-local stability results for the closed-loop system?

In this paper, we design a control law for simultaneously stabilizing and synchronizing oscillations of a desired frequency and amplitude, and with desired phase-shifts between oscillations, in a network of n double integrator systems. Applications of the control law include the presented motivating case of generating a lateral undulatory swimming motion in a USR. The novel control law is based on dynamic consensus control and energy-shaping control, and is shown to render the closed-loop system almost globally asymptotically stable (AGAS). A simulation study is performed, demonstrating the ability of the controller to stabilize and synchronize the desired oscillations with the correct phase shifts between oscillators.

The paper is structured as follows: In Section II we present some preliminary material which will be used throughout the control design and analysis. Following this, we give a description of the control problem and present the proposed control law in Section III. Then, in Section IV we perform a stability analysis of the system under the proposed controller, before presenting our main result. Following this, we present a simulation study demonstrating the stability of the desired orbit of the closed-loop system in Section V. Finally, in Section VI, we conclude and discuss future work.

II. PRELIMINARIES

We now present some preliminaries which will be used in the control design and subsequent proof.

A. Notation

1) *Hadamard product and Hadamard power*: The Hadamard product between two vectors $\mathbf{a}, \mathbf{b} \in \mathbb{R}^n$ is defined as

$$\mathbf{a} \odot \mathbf{b} = [a_1 b_1, a_2 b_2, \dots, a_n b_n]^T \quad (1)$$

where a_i, b_i are the i -th elements of \mathbf{a}, \mathbf{b} , respectively. Analogously, the i -th Hadamard power of a vector $\mathbf{a} \in \mathbb{R}^n$ is defined as

$$\mathbf{a}^{\circ i} = [a_1^i, a_2^i, \dots, a_n^i]^T. \quad (2)$$

2) *Projection Matrix*: A projection matrix, denoted $\mathbf{\Pi}$, is a matrix that maps a vector $\mathbf{x} \in \mathbb{R}^n$ to a subspace V of \mathbb{R}^n . The matrix $\mathbf{\Pi}$ is symmetric. The subspace to which $\mathbf{\Pi}$ projects is an eigenspace of $\mathbf{\Pi}$ with eigenvalue 1, and V^\perp is an eigenspace of $\mathbf{\Pi}$ with eigenvalue 0. Moreover, its eigenspaces imply that it is positive semidefinite and idempotent, that is, $\mathbf{\Pi}^2 = \mathbf{\Pi}$.

B. The lateral undulation gait

As described in [4], the lateral undulation gait of an n -joint snake-like robot is described by the desired trajectories for the joint angles ϕ_i :

$$\phi_i(t) = \alpha_d \sin(\omega t - (i-1)\varphi) + \phi_0 \quad \forall i \in \{1 \dots n\} \quad (3)$$

where $\alpha_d > 0$ is the desired amplitude of the oscillation of each joint, ω is the desired frequency, and φ is the desired phase shift between two joints. The parameter ϕ_0 , known as the turning coefficient, is an offset which will result in a curving of the overall body of the snake-like robot, and which is responsible for causing the robot to turn during locomotion. As described in Section I, a possible alternative to an explicit sinusoidal expression for generating gait patterns is the use of CPGs as in [11]–[13]. However, whether the pattern is given in closed form or generated by a CPG, the closed-loop control consists of trajectory tracking. An alternative approach is to induce the pattern directly into the dynamics of the snake-like robot, using the approach of energy-shaping, similar to [15]. The synchronization problem, then, is well described by the framework for studying networked nonlinear systems as presented in [16].

C. From consensus to synchronization

As described in [17], dynamic consensus may arise in identical nonlinear oscillators under a distributed consensus-control law. Similarly to the networked dynamic consensus framework described in [16], generating and stabilizing a lateral undulation gait in a snake-like robot can be formulated as stabilizing and synchronizing each joint to a mean-field behavior. However, in our case we require the behavior of each joint to be synchronized up to a phase shift, as opposed to achieving consensus. Furthermore, the consensus control law as proposed in [16] requires full control authority, which is not present in mechanical systems, where we are only able to directly control accelerations. Still, consider first a motivating example.

Example. In the literature on consensus control, a system is analyzed by projecting the state onto two orthogonal subspaces. The first part of this decomposition is denoted the mean-field behavior, while the second is denoted the synchronization errors. While the most well-known case in the literature occurs by generating a single mean-field behavior, (see, for instance, [16]), we consider now the case when two orthonormal vectors $\mathbf{v}_1, \mathbf{v}_2$ form the basis for this subspace. The subspace on which the synchronization errors evolve is then the orthogonal complement of the span of $\mathbf{v}_1, \mathbf{v}_2$. We use these vectors to form the matrix $\mathbf{H} = [\mathbf{v}_1, \mathbf{v}_2]$. Subsequently, we construct a projection matrix $\mathbf{\Pi} = \mathbf{I} - \mathbf{H}\mathbf{H}^\top$ which maps the state of a system to the synchronization errors. For $2n$ one-dimensional interconnected systems we denote the overall state as \mathbf{x} , and we define the synchronization errors $\mathbf{e}_x = \mathbf{\Pi}\mathbf{x}$ and the mean-field behavior $\mathbf{x}_s = \mathbf{H}^\top\mathbf{x}$. We note that the synchronization error is defined in excessive coordinates while the mean-field behavior is in condensed coordinates, as is typical in the literature on consensus control. We may recast \mathbf{x}_s back to excessive coordinates in order to reconstruct our original system state as $\mathbf{x} = \mathbf{e}_x + \mathbf{H}\mathbf{x}_s$.

Consider now the network of $2n$ interconnected systems with the overall dynamics

$$\dot{\mathbf{x}} = -\mathbf{\Pi}\mathbf{x} \quad (4)$$

Using the fact that $\mathbf{\Pi}$ is idempotent and that $\mathbf{H}^\top\mathbf{\Pi} \equiv \mathbf{0}$, we may write the dynamics of the decomposition of the system (4) as

$$\dot{\mathbf{e}}_x = -\mathbf{e}_x, \quad (5a)$$

$$\dot{\mathbf{x}}_s = \mathbf{0}. \quad (5b)$$

We note that the subsystem (5a) is UGES. However, the mean-field behavior stays constant throughout. Thus in this case we see that each system state of (4) converges to a different linear combination of the initial condition of \mathbf{x} , specifically, $\mathbf{x}(t)$ converges to $\mathbf{H}\mathbf{H}^\top\mathbf{x}(0)$. \blacktriangle

Having seen this simple motivating example, we now introduce a system of n linear oscillators under a control \mathbf{w} :

$$\dot{\mathbf{y}}_1 = \omega\mathbf{y}_2, \quad (6a)$$

$$\dot{\mathbf{y}}_2 = -\omega\mathbf{y}_1 + \mathbf{w}, \quad (6b)$$

and we write $\mathbf{y}_1 = [y_{1,1}, \dots, y_{1,n}]^\top$, $\mathbf{y}_2 = [y_{2,1}, \dots, y_{2,n}]^\top$. Furthermore, we refer to the subsystem of (6) with state $(y_{1,i}, y_{2,i})$ as oscillator i .

Motivated by the methodology of [16] we project the system dynamics (6) onto two orthogonal subspaces. The first projection captures a mean-field behavior of the network \mathbf{y}_s , while the second component captures the synchronization errors \mathbf{e} , the deviation from the phase-shifted mean-field behavior of each system.

To this end, we introduce the vectors

$$\mathbf{c} = \sqrt{\frac{1}{n}} [1, \cos(\varphi), \dots, \cos((n-1)\varphi)]^\top \in \mathbb{R}^n, \quad (7a)$$

$$\mathbf{s} = \sqrt{\frac{1}{n}} [0, \sin(\varphi), \dots, \sin((n-1)\varphi)]^\top \in \mathbb{R}^n,$$

$$\mathbf{v}_1 = [\mathbf{c}^\top, \mathbf{s}^\top]^\top \in \mathbb{R}^{2n}, \quad \mathbf{v}_2 = [-\mathbf{s}^\top, \mathbf{c}^\top]^\top \in \mathbb{R}^{2n}. \quad (7b)$$

Furthermore, we define the matrix $\mathbf{H} = [\mathbf{v}_1 \mathbf{v}_2] \in \mathbb{R}^{2n \times 2}$. We note that the vectors $\mathbf{v}_1, \mathbf{v}_2$ form an orthonormal basis for a 2-dimensional subspace from which a decomposition of (6) can be defined.

Thus, we define the projection matrix:

$$\mathbf{\Pi} = \mathbf{I}_{2n} - \mathbf{H}\mathbf{H}^\top \in \mathbb{R}^{2n \times 2n} \quad (8a)$$

which projects \mathbf{y} to the synchronization error subspace. We note that $\mathbf{\Pi}$ has a block structure

$$\mathbf{\Pi} = \begin{bmatrix} \mathbf{\Pi}_1 & \mathbf{\Pi}_2^\top \\ \mathbf{\Pi}_2 & \mathbf{\Pi}_1 \end{bmatrix}$$

where $\mathbf{\Pi}_1 = \mathbf{\Pi}_1^\top \geq 0$, and $\mathbf{\Pi}_2 = -\mathbf{\Pi}_2^\top$.

Furthermore, we define the following:

$$\mathbf{y}_s = \mathbf{H}^\top\mathbf{y} \in \mathbb{R}^2, \quad (9a) \quad \mathbf{e} = \mathbf{\Pi}\mathbf{y} \in \mathbb{R}^{2n}, \quad (9b)$$

We write $\mathbf{e} = [\mathbf{e}_1^\top, \mathbf{e}_2^\top]^\top$ with $\mathbf{e}_1 = [e_{1,1}, \dots, e_{1,n}]^\top$, $\mathbf{e}_2 = [e_{2,1}, \dots, e_{2,n}]^\top$. We also note that the synchronization errors \mathbf{e} are kept in excessive coordinates due to their use in the control implementation.

Due to the control input in (6) being restricted to \mathbf{y}_2 , we consider an altered structure for the consensus controller. We choose \mathbf{w} in (6) as $\mathbf{w} = -\sigma\mathbf{\Pi}_2\mathbf{y}_1 - \sigma\mathbf{\Pi}_1\mathbf{y}_2$, corresponding to the lower half of $-\mathbf{\Pi}\mathbf{y}$ multiplied by a coupling gain σ . The dynamics of the decomposition of (6) under this control input become

$$\dot{\mathbf{e}}_1 = \omega\mathbf{e}_2 - \sigma\mathbf{\Pi}_2^\top\mathbf{e}_2 \quad (10a)$$

$$\dot{\mathbf{e}}_2 = -\omega\mathbf{e}_1 - \sigma\mathbf{\Pi}_1\mathbf{e}_2 \quad (10b)$$

$$\dot{y}_{s,1} = \omega y_{s,2} - \sigma\mathbf{s}^\top\mathbf{e}_2 \quad (10c)$$

$$\dot{y}_{s,2} = -\omega y_{s,1} - \sigma\mathbf{c}^\top\mathbf{e}_2 \quad (10d)$$

We now introduce the Lyapunov function candidate $V_e(\mathbf{e}) = \frac{1}{2}\mathbf{e}^\top\mathbf{e}$ and consider its derivative:

$$\begin{aligned} \dot{V}_e(\mathbf{e}) &= \omega\mathbf{e}_1^\top\mathbf{e}_2 - \sigma\mathbf{e}_1^\top\mathbf{\Pi}_2^\top\mathbf{e}_2 - \omega\mathbf{e}_2^\top\mathbf{e}_1 - \sigma\mathbf{e}_2^\top\mathbf{\Pi}_1\mathbf{e}_2 \\ &= -\sigma\|\mathbf{e}_2\|^2 \end{aligned}$$

from which we can conclude that the subsystem Eqs. (10a) and (10b) is globally stable (GS) and that \mathbf{e}_2 converges to zero, using Barbalat's lemma. From Eqs. (10a) and (10b), using Barbashin-Krasovskii-LaSalle, we may conclude that the origin of the subsystem Eqs. (10a) and (10b) is globally asymptotically stable (GAS).

We note that there also exists a Lyapunov function candidate $V_{e,2}(\mathbf{e}) = V_e(\mathbf{e}) + \frac{\sigma^2}{4\omega^2}\mathbf{e}_1^\top\mathbf{\Pi}_1\mathbf{e}_1 + \frac{\sigma}{2\omega}\mathbf{e}_1^\top\mathbf{e}_2$ with $\dot{V}_{e,2}(\mathbf{e}) \leq -\frac{\sigma}{2}\|\mathbf{e}\|^2$ which can be used to show that the system given by Eqs. (10a) and (10b) is UGES. However, due to space limitations, the derivations are omitted here.

It is clear from (10) that when $\mathbf{e} = \mathbf{0}$ the \mathbf{y}_s -subsystem behaves like a single linear oscillator with the desired frequency ω and some amplitude $\bar{\alpha}$. Moreover, from $\mathbf{y} = \mathbf{H}\mathbf{y}_s + \mathbf{\Pi}\mathbf{e}$, we see that when $\mathbf{e} = \mathbf{0}$, each oscillator subsystem i of (6) with state $(y_{1,i}, y_{2,i})$ is a linear combination of $\mathbf{y}_{s,1}, \mathbf{y}_{s,2}$ with weights given by the rows i and $i+n$ of the matrix \mathbf{H} . The result is that the solution of each oscillator i is an oscillation with amplitude $\bar{\alpha}$ and frequency ω , but with the phase difference between adjacent oscillators equal to φ .

III. PROBLEM DESCRIPTION AND CONTROL DESIGN

Our control objective is to generate and stabilize a lateral undulation gait, given by the pattern in (3), in an n -joint USR. While the frequency in general can be non-constant, we restrict ourselves in this paper to the case of a constant desired frequency ω and where the turning coefficient ϕ_0 is 0. Furthermore, we choose the desired phase shift as $\varphi = \frac{2\pi}{n}$.

A. Problem description

As shown in [18], through a suitable feedback-linearizing controller, the joint dynamics of an n -joint USR can be reduced to a system of n double integrators. Thus, we consider a system of n double integrators

$$\dot{\mathbf{x}}_1 = \mathbf{x}_2 \quad (11a)$$

$$\dot{\mathbf{x}}_2 = \mathbf{u} \quad (11b)$$

with state $\mathbf{x} = [\mathbf{x}_1^\top, \mathbf{x}_2^\top]^\top \in \mathbb{R}^{2n}$, $\mathbf{x}_1 = [x_{1,1}, \dots, x_{1,n}]^\top \in \mathbb{R}^n$, $\mathbf{x}_2 = [x_{2,1}, \dots, x_{2,n}]^\top \in \mathbb{R}^n$, and where $\mathbf{u} \in \mathbb{R}^n$ is our control

input. Here, \mathbf{x}_1 corresponds to the joint angles of the USR, while \mathbf{x}_2 corresponds to the joint angle velocities of the USR.

The control objective of generating and stabilizing a lateral undulation gait in the USR, is then equivalent to stabilizing each system of double integrators with state $(x_{1,i}, x_{2,i})$ to the orbit (as defined in [19]) of a linear oscillation with the same properties as that of the lateral undulation gait, while simultaneously stabilizing the phase angle difference between oscillations to the desired phase shift φ . The first of these control objectives may be reformulated as asymptotically stabilizing the system (11) to some set \mathcal{O}_x , the desired orbit. The second objective may be recast as a synchronization problem of a network of dynamical systems.

To this end, we choose our input \mathbf{u} to be

$$\mathbf{u} = -\omega^2\mathbf{x}_1 + \omega\mathbf{w}, \quad (12)$$

where \mathbf{w} is a virtual control signal to be designed.

We see that by performing a change of variables to $\mathbf{y}_1 = \mathbf{x}_1$, $\mathbf{y}_2 = \frac{1}{\omega}\mathbf{x}_2$, our system (11) is transformed to the system (6) under a virtual control \mathbf{w} .

B. Control Design

We are now ready to present our proposed control law. We desire to achieve two separate control objectives simultaneously. Firstly, we desire to control all oscillators of the system (6) to linear oscillations with magnitude α_d and frequency ω . To this end, we introduce the virtual energy of oscillator i of (6), $E_i = \frac{\omega^2}{2}(y_{1,i}^2 + y_{2,i}^2)$. For an oscillator with a constant frequency and amplitude, the amplitude can be expressed as $\alpha = \frac{\sqrt{2E}}{\omega}$ where E is the energy of the oscillator. Given that the frequency of the oscillator is ω , we may thus replace the control objective of stabilizing the amplitude to α_d with the objective of stabilizing the oscillator to a desired virtual energy $E_d = \frac{\omega^2\alpha_d^2}{2}$.

Secondly, we wish to synchronize the oscillators so that adjacent oscillators have the phase shift φ . In order to achieve both of these control objectives simultaneously, we propose the following virtual control law:

$$\mathbf{w} = \mathbf{w}_E + \mathbf{w}_S \quad (13a)$$

where

$$\mathbf{w}_E = -K\mathbf{y}_2 \odot \left(\frac{\omega^2}{2}(\mathbf{y}_1^{\circ 2} + \mathbf{y}_2^{\circ 2}) - E_d\mathbf{1} \right) \quad (13b)$$

$$\mathbf{w}_S = -\sigma\mathbf{\Pi}_2\mathbf{y}_1 - \sigma\mathbf{\Pi}_1\mathbf{y}_2 \quad (13c)$$

and where $K \in \mathbb{R}$ and $\sigma \in \mathbb{R}$ are tuning parameters.

As a result the closed-loop system takes the form

$$\dot{\mathbf{y}}_1 = \omega\mathbf{y}_2 \quad (14a)$$

$$\begin{aligned} \dot{\mathbf{y}}_2 &= -\omega\mathbf{y}_1 - K\mathbf{y}_2 \odot \left(\frac{\omega^2}{2}(\mathbf{y}_1^{\circ 2} + \mathbf{y}_2^{\circ 2}) - E_d\mathbf{1} \right) \\ &\quad - \sigma\mathbf{\Pi}_2\mathbf{y}_1 - \sigma\mathbf{\Pi}_1\mathbf{y}_2. \end{aligned} \quad (14b)$$

The term (13b), which contributes to stabilizing the amplitude of each oscillator, is motivated by control laws from the literature on energy shaping, such as [20].

We now introduce the virtual energy error state

$$\tilde{\mathbf{E}} = \mathbf{E} - E_d\mathbf{1}, \quad (15)$$

where $\mathbf{E} = [E_1, \dots, E_n]^\top \in \mathbb{R}^n$, with the closed-loop dynamics

$$\dot{\tilde{\mathbf{E}}} = -\omega^2 K \mathbf{y}_2^{\circ 2} \tilde{\mathbf{E}} - \omega^2 \sigma \mathbf{y}_2 \odot \mathbf{e}_2, \quad (16)$$

and we note that $\tilde{\mathbf{E}} = \mathbf{0}$ if and only if $\mathbf{y} \in \mathcal{O}_y$ defined as

$$\mathcal{O}_y = \{\mathbf{y} = [\mathbf{y}_1^\top, \mathbf{y}_2^\top]^\top \in \mathbb{R}^{2n} \mid y_{1,i}^2 + y_{2,i}^2 = \alpha_d^2\} \quad (17)$$

$\forall i \in \{1 \dots n\}$. Clearly, $\mathbf{y} \in \mathcal{O}_y$ implies that all $y_{1,i}, y_{2,i}$ stay on the circular orbit of radius α_d .

The stabilizing term in (16) originates from (13b), motivating its inclusion in (13).

The term (13c), which contributes to the synchronization of the network of oscillators, is motivated by control laws from the literature on dynamic consensus of networked systems, such as [16], although alterations are made due to the lack of full control authority in the system (6). The analysis of (10) in Section II-C motivates the inclusion of (13c) in (13).

IV. STABILITY ANALYSIS

In this section we present results on the stability analysis of the closed-loop system (14). The controller satisfies two separate control objectives at once. Firstly, it shapes the virtual energy of the oscillators in order to achieve a desired amplitude α_d , that is, to stabilize the set \mathcal{O}_y . Secondly, it drives the synchronization errors $\mathbf{e}(t)$ asymptotically to zero. When the first objective is achieved, the system (14) is equivalent to (10). Thus, when both control objectives are satisfied simultaneously, they ensure both the stabilization of an orbit with the desired frequency and amplitude, and the synchronization to the desired phase shift. We will make these notions more rigorous in what follows.

We start this section with two auxiliary statements on the behavior of the system constrained to the set \mathcal{O}_y . Next we prove the global attractivity of the invariant set

$$\mathcal{S}_\xi = \left\{ \mathbf{y} \in \mathbb{R}^{2n} \mid \left(\mathcal{O}_y \cap \{ \mathbf{y} \in \mathbb{R}^{2n} \mid \mathbf{e} = \mathbf{0} \} \right) \cup \{ \mathbf{0} \} \right\} \quad (18)$$

under the proposed virtual control law (13). Finally we prove that the set $\mathcal{S}_\xi \setminus \{ \mathbf{0} \}$ is AGAS for the closed-loop system (14).

We now state some properties of the system which relate to the mean-field behavior of (10) in the limit. However, we note that these results hold not only for (6) under (13c), but under (13). We propose the following:

Proposition 1. *Assume that the solution to each oscillator i of (6) is a linear oscillation with the constant frequency ω and with the constant positive amplitude α_i . Then, the solution to the mean-field behavior, $\mathbf{y}_s(t)$, is a linear oscillator with the frequency ω , an amplitude $\sqrt{n}\bar{\alpha} \geq 0$, and a phase-shift $\bar{\lambda}$. Furthermore, $\mathbf{e} = \mathbf{0}$ if and only if all α_i are equal to $\bar{\alpha}$ and the phase of each oscillator is $\lambda_i = \bar{\lambda} - (i-1)\varphi \forall i \in \{1 \dots n\}$.*

Proof. Under the stated assumptions, we have that

$$\begin{aligned} \mathbf{y}_s(t) &= \mathbf{H}^\top \mathbf{y}(t) = \sqrt{\frac{1}{n}} \begin{bmatrix} \sum_{i=1}^{n-1} \alpha_i \sin(\omega t + \lambda_i + (i-1)\varphi) \\ \sum_{i=1}^{n-1} \alpha_i \cos(\omega t + \lambda_i + (i-1)\varphi) \end{bmatrix} \\ &\triangleq \sqrt{n}\bar{\alpha} \begin{bmatrix} \sin(\omega t + \bar{\lambda}) \\ \cos(\omega t + \bar{\lambda}) \end{bmatrix} \end{aligned} \quad (19)$$

where λ_i is the phase of oscillator i . Under the constraint $\bar{\alpha} \geq 0$, the values of $\bar{\alpha}, \bar{\lambda}$ satisfying (19) are unique.

Furthermore, if $e_{1,i}(t) = 0, e_{2,i}(t) = 0 \forall i \in \{1 \dots n\}$, considering $\mathbf{e} = \mathbf{y} - \mathbf{H}\mathbf{y}_s$, we have that

$$\begin{aligned} y_{1,i}(t) &= \bar{\alpha} (\cos((i-1)\varphi) \sin(\omega t + \bar{\lambda}) - \sin((i-1)\varphi) \cos(\omega t + \bar{\lambda})) \\ &= \bar{\alpha} \sin(\omega t + \bar{\lambda} - (i-1)\varphi), \\ y_{2,i}(t) &= \bar{\alpha} (\cos((i-1)\varphi) \cos(\omega t + \bar{\lambda}) + \sin((i-1)\varphi) \sin(\omega t + \bar{\lambda})) \\ &= \bar{\alpha} \cos(\omega t + \bar{\lambda} - (i-1)\varphi), \end{aligned}$$

which, given $\alpha_i, \bar{\alpha} \geq 0$, implies that

$$\alpha_i = \bar{\alpha}, \lambda_i = \bar{\lambda} - (i-1)\varphi \quad \forall i \in \{1 \dots n\}$$

■

We note here that for the system (6) under (13c), $\mathbf{e} = \mathbf{0}$ is sufficient for the assumption of Proposition 1 to be satisfied, while this is not the case for the system (14).

Remark. *As $\mathbf{y} \in \mathcal{O}_y$ if and only if $\tilde{\mathbf{E}} = \mathbf{0}$, an equivalent reformulation of the set $\mathcal{S}_\xi \setminus \{ \mathbf{0} \}$ is*

$$\mathcal{S}_\xi \setminus \{ \mathbf{0} \} = \{ \mathbf{y} \in \mathbb{R}^{2n} \mid \mathbf{e} = \mathbf{0}, \tilde{\mathbf{E}} = \mathbf{0} \}. \quad (20)$$

To help us show the AGAS of the set $\mathcal{S}_\xi \setminus \{ \mathbf{0} \}$ for the system (14), we now propose the following:

Proposition 2. *Consider the system (14), and let K in (13b) be chosen as $K = \frac{\sigma}{E_d} (1 - \varepsilon)$, where $\varepsilon \in (0, 1)$. Then the auxiliary variable $\xi = \frac{K}{\sigma} \mathbf{y}_2 \odot \tilde{\mathbf{E}} + \mathbf{e}_2$ converges to zero along all solutions of the system (14). Furthermore, the set \mathcal{S}_ξ can be reformulated as $\mathcal{S}_\xi = \{ \mathbf{y} \in \mathbb{R}^{2n} \mid \|\xi\| = 0 \}$. Thus, \mathcal{S}_ξ is a globally attractive set of the system (14).*

Proof. Consider the following Lyapunov function candidate

$$V(\mathbf{e}, \tilde{\mathbf{E}}) = \frac{1}{2} \mathbf{e}^\top \mathbf{e} + \frac{K}{2\omega^2 \sigma} \tilde{\mathbf{E}}^\top \tilde{\mathbf{E}},$$

notice that the first term coincides with the Lyapunov function that we previously proposed for the analysis of system (6). Derivating $V(\mathbf{e}, \tilde{\mathbf{E}})$ along solutions of the system (14) we obtain

$$\begin{aligned} \dot{V}(\mathbf{e}, \tilde{\mathbf{E}}) &= \omega \mathbf{y}_1^\top \mathbf{\Pi}_1 \mathbf{y}_2 - \omega \mathbf{y}_2^\top \mathbf{\Pi}_1 \mathbf{y}_1 - K \mathbf{y}_2^\top \mathbf{\Pi}_1 \mathbf{y}_2 \odot \tilde{\mathbf{E}} - \sigma \mathbf{y}_2^\top \mathbf{\Pi}_1 \mathbf{e}_2 \\ &\quad + \omega \mathbf{y}_2^\top \mathbf{\Pi}_2 \mathbf{y}_2 - \omega \mathbf{y}_1^\top \mathbf{\Pi}_2 \mathbf{y}_1 - K \mathbf{y}_1^\top \mathbf{\Pi}_2 \mathbf{y}_2 \odot \tilde{\mathbf{E}} - \sigma \mathbf{y}_1^\top \mathbf{\Pi}_2 \mathbf{e}_2 \\ &\quad - \frac{K^2}{\sigma} \mathbf{y}_2^{\circ 2} \odot \tilde{\mathbf{E}}^\top \tilde{\mathbf{E}} - K \tilde{\mathbf{E}}^\top \mathbf{y}_2 \odot \mathbf{e}_2 \\ &= -\sigma \mathbf{e}_2^\top \mathbf{e}_2 - \frac{K^2}{\sigma} (\mathbf{y}_2 \odot \tilde{\mathbf{E}})^\top (\mathbf{y}_2 \odot \tilde{\mathbf{E}}) - 2K \mathbf{e}_2^\top (\mathbf{y}_2 \odot \tilde{\mathbf{E}}) \\ &= -\sigma \|\xi\|^2 \leq 0 \end{aligned}$$

where we have used the fact that $\mathbf{e}^\top \mathbf{e} = \mathbf{y}^\top \mathbf{\Pi} \mathbf{y}$.

Next, to show that asymptotically $\xi(t) \rightarrow \mathbf{0}$, we use Barbalat's Lemma. First, since the derivative of the Lyapunov function is negative semi-definite, we have that all solutions

to (14) are globally bounded. Furthermore, $\frac{d^2}{dt^2}V(\mathbf{e}(t), \tilde{\mathbf{E}}(t))$ consists only of terms which depend continuously on $\mathbf{y}(t)$, thus $\frac{d^2}{dt^2}V(\mathbf{e}(t), \tilde{\mathbf{E}}(t))$ is bounded. Hence we conclude that $\dot{V}(\mathbf{e}(t), \tilde{\mathbf{E}}(t)) \rightarrow 0$, and therefore that $\|\xi\| \rightarrow 0$, as $t \rightarrow \infty$.

Restricting the dynamics of (14) on the set where $\|\xi\| = 0$, we obtain that either it reduces to (6) with $\mathbf{w} = 0$, or $\|\mathbf{y}\| = 0$. If $\|\mathbf{y}\| \neq 0$, it behaves as a linear oscillator with constant frequency ω , phase shift λ_i and constant nonnegative amplitude $\alpha_i = \sqrt{y_{1,i}(t)^2 + y_{2,i}(t)^2}$. This also implies that \mathbf{E} is constant. Recalling that $K = \frac{\sigma}{E_d} (1 - \varepsilon)$, we may reformulate $\xi = \mathbf{0}$ as

$$\left(\varepsilon \mathbf{1} + \frac{(1-\varepsilon)\omega^2}{2E_d} (\mathbf{y}_1^{\circ 2} + \mathbf{y}_2^{\circ 2}) \right) \odot \mathbf{y}_2 = [\mathbf{0}_{n \times n} \quad \mathbf{I}_n] \mathbf{H} \mathbf{y}_s$$

and considering that the assumptions of Proposition 1 are satisfied, substituting the solutions to (6) with $\mathbf{w} \equiv 0$ yields

$$\left(\varepsilon + (1-\varepsilon) \frac{\alpha_i^2}{\alpha_d^2} \right) \alpha_i \cos(\omega t + \lambda_i) = \bar{\alpha} \cos(\omega t + \bar{\lambda} - (i-1)\varphi) \quad (21)$$

$\forall i \in \{1 \dots n\}$.

As we now assume $\|\mathbf{y}\| \neq 0$, we have $\bar{\alpha} > 0$. Thus, we have that

$$\begin{aligned} & \left(\varepsilon + (1-\varepsilon) \frac{\alpha_i^2}{\alpha_d^2} \right) \alpha_i \cos(\omega t + \lambda_i + (i-1)\varphi) \\ &= \left(\varepsilon + (1-\varepsilon) \frac{\alpha_j^2}{\alpha_d^2} \right) \alpha_j \cos(\omega t + \lambda_j + (j-1)\varphi) \quad \forall i, j. \end{aligned}$$

This again implies

$$\begin{aligned} \left(\varepsilon + (1-\varepsilon) \frac{\alpha_i^2}{\alpha_d^2} \right) \alpha_i &= \left(\varepsilon + (1-\varepsilon) \frac{\alpha_j^2}{\alpha_d^2} \right) \alpha_j, \\ \lambda_i + (i-1)\varphi &= \lambda_j + (j-1)\varphi = \bar{\lambda}, \end{aligned}$$

which, for $\alpha_i, \alpha_j \geq 0$ implies $\alpha_i = \alpha_j = \alpha^* \quad \forall i, j$. Inserting this into (19), we arrive at $\bar{\alpha} = \alpha^*$. Substituting back into (21), we see that the only solution is $\alpha^* = \alpha_d$. As $\lambda_i = \bar{\lambda} - (i-1)\varphi$, $\alpha_i = \alpha_d \quad \forall i$, we see in this case that $\mathbf{y}(t) \in \mathcal{S}_\xi \setminus \{\mathbf{0}\}$. ■

We are now ready to present the main result of our paper:

Theorem 1. *The set $\mathcal{S}_\xi \setminus \{\mathbf{0}\}$ of the system (14) with K chosen as in Proposition 2 is AGAS. Thus, a corresponding set $\mathcal{S}_x = \{\mathbf{x} \in \mathbb{R}^{2n} \mid \mathbf{e} = \mathbf{0}, \tilde{\mathbf{E}} = \mathbf{0}\}$ of the system (11) in closed loop with the controller (12) is also AGAS.*

Due to space limitations we present here only a sketch of the proof.

In Proposition 2 we have shown the set \mathcal{S}_ξ is globally attractive. This implies that all solutions of the system (14) converge either to the set $\mathcal{S}_\xi \setminus \{\mathbf{0}\}$ or to the origin. Also, direct but tedious calculations show that the invariant set of the mean-field model of the closed-loop system is composed of an almost globally asymptotically stable orbit and an unstable equilibrium point (the origin). Then, to show that the set $\mathcal{S}_\xi \setminus \{\mathbf{0}\}$ is almost globally asymptotically stable for the system (14) we are left only to show that all initial conditions $\mathbf{y}(0)$ such that trajectories starting from them converge to the origin, form a set of measure zero.

To prove this we proceed as follows. First, it can be shown that the linearization at the origin of the system (14) has $2n-2$

eigenvalues in the left half-plane, and only 2 eigenvalues in the right half-plane (corresponding to the dynamics of \mathbf{y}_s). This implies that the origin is a hyperbolic equilibrium. Then using the stable manifold theorem [21, Theorem 13.4.1] we show the existence of unique local stable manifold $W^s(\mathbf{0})$ of dimension $2n-2$ and a unique local unstable manifold $W^u(\mathbf{0})$ of dimension 2.

Since any solution to (14) that converges to the origin must enter at some time t_0 the local stable manifold $W^s(0)$, the set of solutions converging to the origin originate from the backward propagation of $W^s(0)$, defined as follows:

$$R(W^s(\mathbf{0})) = \{\mathbf{y}(t) \mid t \leq t_0, \mathbf{y}(t_0) \in W^s(0), \mathbf{y}(\cdot) \text{ sol. to (14)}\} \quad (22)$$

Using the same arguments as in the proof of [22, Theorem 2], it can be shown that the set $R(W^s(\mathbf{0}))$ is a null measure set. As all solutions converging to the origin start from a null measure set, and as \mathcal{S}_ξ is globally attractive from Proposition 2 and the orbit of the mean-field dynamics is locally stable, we conclude that the set $\mathcal{S}_\xi \setminus \{\mathbf{0}\}$ is almost globally attractive and stable. Thus, $\mathcal{S}_\xi \setminus \{\mathbf{0}\}$ is an AGAS orbit of (14). As (11) and \mathcal{S}_x are related to (6) and $\mathcal{S}_\xi \setminus \{\mathbf{0}\}$ through a global diffeomorphism, \mathcal{S}_x is an AGAS orbit of (11).

V. SIMULATION RESULTS

We now present the results of a simulation study which demonstrates the behavior of the system (11) in closed loop with the control law given by (12) and (13). For the study, we chose to simulate $n = 5$ double integrators. We chose a desired frequency $\omega = 2$, a desired amplitude $\alpha_d = 1$, and a desired phase shift $\varphi = \frac{2\pi}{n}$. For tuning parameters, we chose $\sigma = 4$, and $K = 0.6$. We selected the initial conditions to be randomly distributed but fairly far away from the orbit, in order to better demonstrate the almost global properties of the controller.

The time series of the solutions of the system (11), which are shown in Figs. 1a and 1b, demonstrate that the system behavior converges to an oscillatory behavior with the correct desired characteristics within 7 seconds. Figs. 1d to 1f further support this, while illuminating some of the transient characteristics of the system under the proposed controller. We see in Figs. 1d and 1e that the synchronization errors grow temporarily in the transient phase before converging to zero. Firstly, this is explained by the fact that when the magnitude of the configuration variables \mathbf{x}_1 and velocities \mathbf{x}_2 are small, the synchronization errors may be small in absolute terms, even if they are large relative to the magnitude of the states. As the energy increases, and thus the magnitude of the states, the synchronization errors may increase in absolute terms even if they decrease in relative terms. Secondly, the dual objectives of synchronizing the oscillator phases and shaping their energy may be conflicting in the transient phase. Thus, a trade-off occurs where one of the errors may temporarily increase while the other decreases, before both converge to zero.

In Fig. 2 we illustrate the evolution of the states in the phase space through snapshots of the phase portraits of the

oscillator state \mathbf{y} . We have chosen to depict the phase portrait of the state of (6) instead of that of (11) due to the amplitude being uniform in \mathbf{y}_1 and \mathbf{y}_2 on the orbit. Here, we note that the oscillators distribute evenly on an ellipsoid in the phase space also before they reach the orbit in full, which can be seen clearly from $t = 3$.

VI. CONCLUSION AND FUTURE WORK

In this paper, we have presented a control law for stabilizing n coupled linear oscillators to a desired amplitude, and with a desired phase shift between each oscillator. The control law was shown to almost globally asymptotically stabilize the system to the desired orbit while simultaneously stabilizing the synchronization error to the origin, thus synchronizing the orbits to the desired phase shift. Furthermore, a simulation study was presented, which illustrated the properties of the proposed control law by demonstrating the stability of the desired orbit and the synchronization of the closed-loop system. Applications of the control law include the generation and stabilization of undulating gaits in both terrestrial and underwater snake-like robots.

In the future, we would like to apply the proposed control law to generate and stabilize a lateral undulation gait in a USR, and to compare its performance to that of existing reference trajectory tracking controllers from the literature. After testing the controller on a complex nonlinear model of the robot, it would be interesting to implement the controller on a USR in high-fidelity fluid simulations for further verification.

REFERENCES

- [1] J.-L. Wang, J.-L. Song, A.-R. Liu, J.-Q. Liang, F.-B. Zhou, J.-J. Liang, J.-Y. Fu, and B.-C. Chen, "Design and architecture of a slender and flexible underwater robot," *Int. Serv. Robotics*, vol. 17, no. 3, May 2024.
- [2] Y. Qiu and H. Date, "A low computation-cost locomotion control for underwater snake robot based on monte carlo model predictive control and curvature derivative control," *Adv. Rob.*, vol. 38, no. 11, pp. 770–783, Jun. 2024.
- [3] E. Kelasidi, K. Y. Pettersen, J. T. Gravdahl, and P. Liljebäck, "Modeling of underwater snake robots," in *Proc. IEEE Int. Conf. on Rob. and Autom.*, May 2014, pp. 4540–4547.
- [4] E. Kelasidi, P. Liljebäck, K. Y. Pettersen, and J. T. Gravdahl, "Innovation in underwater robots: Biologically inspired swimming snake robots," *IEEE Robotics & Automation Magazine*, vol. 23, no. 1, pp. 44–62, 2016.
- [5] M. Porez, F. Boyer, and A. J. Ijspeert, "Improved lighthill fish swimming model for bio-inspired robots: Modeling, computational aspects and experimental comparisons," *The Int. J. of Rob. Research*, vol. 33, no. 10, pp. 1322–1341, 2014.
- [6] A. Orucevic, J. T. Gravdahl, K. Y. Pettersen, and A. Chaillet, "Uniform practical asymptotic stability for position control of underwater snake robots," eng, *Proc. IEEE Conf. on Control Technology and Applications*, Aug. 2022.
- [7] A. Mohammadi, E. Rezapour, M. Maggiore, and K. Y. Pettersen, "Maneuvering control of planar snake robots using virtual holonomic constraints," *IEEE Trans. on Control Systems Technology*, vol. 24, no. 3, pp. 884–899, 2016.
- [8] M. Maggiore and L. Consolini, "Virtual holonomic constraints for Euler-Lagrange systems," *IEEE Trans. Autom. Control*, vol. 58, no. 4, pp. 1001–1008, 2013.
- [9] B. M. Patel and S. K. Dwivedy, "Virtual holonomic constraints based super twisting sliding mode control for motion control of planar snake robot in the uncertain underwater environment," *Proc. Inst. Mech. Eng., Part I: J. of Sys. and Cont. Eng.*, vol. 237, no. 8, pp. 1480–1491, 2023.
- [10] J. Hauser and R. Hindman, "Maneuver regulation from trajectory tracking: Feedback linearizable systems," en, *IFAC Proc. Vol.*, vol. 28, no. 14, pp. 595–600, Jun. 1995.
- [11] X. Wu and S. Ma, "CPG-based control of serpentine locomotion of a snake-like robot," en, *Mechatronics*, vol. 20, no. 2, pp. 326–334, 2010.
- [12] H. Tamura and T. Kamegawa, "Parameter search of a CPG network using a genetic algorithm for a snake robot with tactile sensors moving on a soft floor," en, *Frontiers in Robotics and AI*, Mar. 2023.
- [13] K. Inoue, T. Sumi, and S. Ma, "Cpg-based control of a simulated snake-like robot adaptable to changing ground friction," en, in *Proc. IEEE/RSJ Int. Conf. Int. Rob. Sys.*, San Diego, CA, Oct. 2007.
- [14] A. J. Ijspeert, "Central pattern generators for locomotion control in animals and robots: A review," *Neural Networks, Robotics and Neuroscience*, vol. 21, no. 4, pp. 642–653, May 2008.
- [15] M. E. B. Lysø, K. Y. Pettersen, and J. T. Gravdahl, "Energy-Shaping Control for Swimming in Underwater Snake Robots," in *Proc. 15th IFAC Conf. Cont. App. Marine Sys., Rob. and Veh.*, Blacksburg, Virginia, USA, Sep. 2024.
- [16] E. Panteley and A. Loria, "Synchronization and dynamic consensus of heterogeneous networked systems," *IEEE Trans. Autom. Control*, vol. 62, no. 8, pp. 3758–3773, 2017.
- [17] A. Lazri, E. Panteley, and A. Loria, "Dynamic consensus of nonlinear oscillators under weak coupling," in *Proc. 25th Math. Th. Net. Sys.*, Bayreuth, Germany, Sep. 2022.
- [18] P. Liljebäck, K. Y. Pettersen, Ø. Stavadahl, and J. T. Gravdahl, "Controllability and stability analysis of planar snake robot locomotion," *IEEE Trans. Autom. Control*, vol. 56, no. 6, pp. 1365–1380, 2010.
- [19] M. Urabe, "Nonlinear autonomous oscillations: Analytical theory," en, *Elsevier*, vol. 34, 1967.

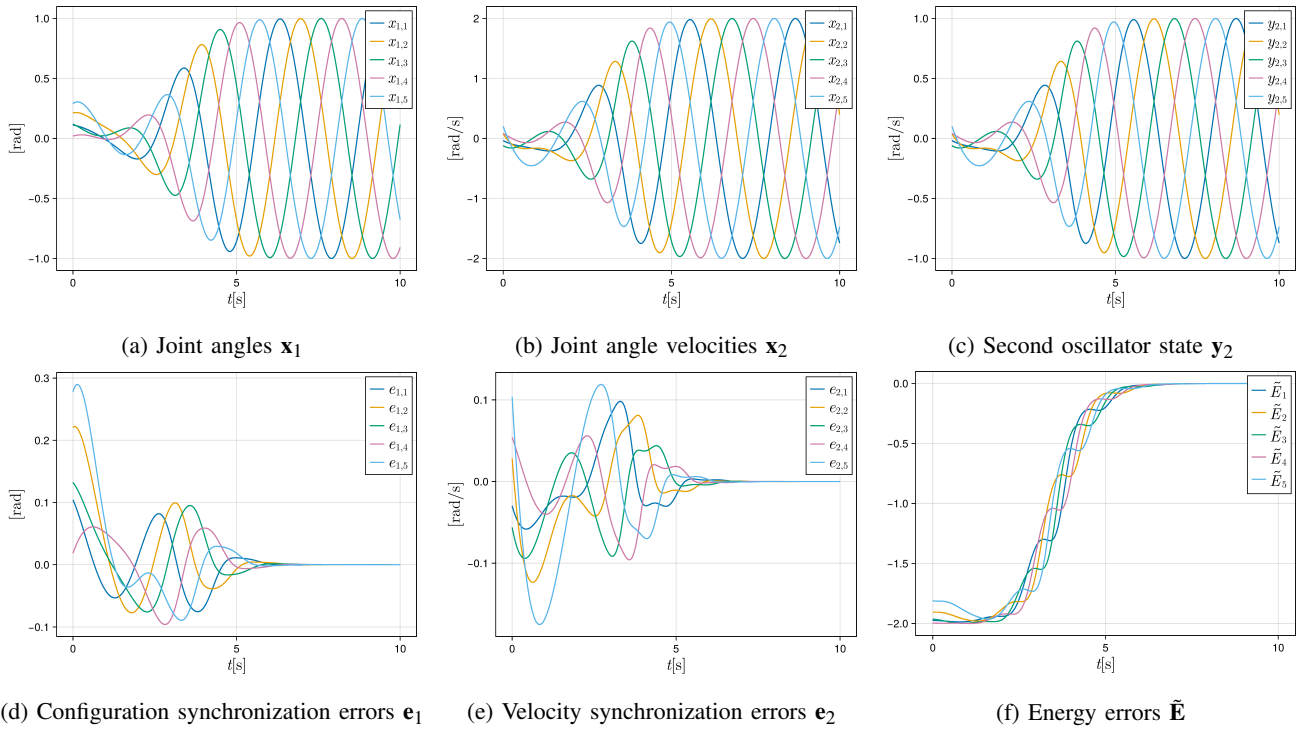


Fig. 1: Plots of the joint angles, synchronization errors and virtual energy errors

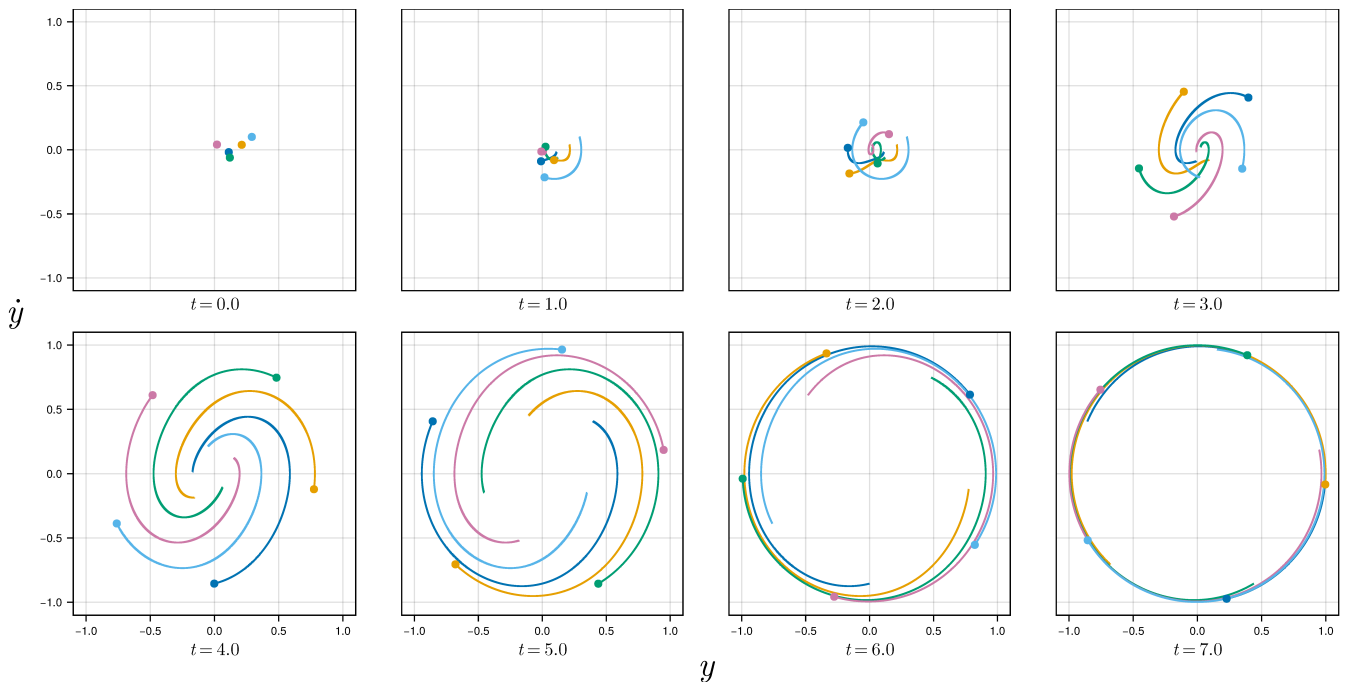


Fig. 2: Snapshots of phase portraits in \mathbf{y} . A graph of the preceding 2 s of the trajectory (with a cutoff at $t = 0$ s) is plotted along with the current state at each snapshot.

- [20] C. C. Chung and J. Hauser, "Nonlinear control of a swinging pendulum," en, *Automatica*, vol. 31, no. 6, pp. 851–862, 1995.
- [21] E. A. Coddington and N. Levinson, *Theory of Ordinary Differential Equations*. McGraw-Hill, 1955.
- [22] M. Maghenem, E. Panteley, and A. Loria, "Singular-perturbations-based analysis of dynamic consensus in directed networks of heterogeneous nonlinear systems," *IEEE Trans. Autom. Control*, pp. 1–16, 2023.